

See discussions, stats, and author profiles for this publication at: <https://www.researchgate.net/publication/259964029>

Theoretical Insights into Adsorption of Cobalt Phthalocyanine on Ag(111): A Combination of Chemical and van der Waals Bonding

ARTICLE *in* THE JOURNAL OF PHYSICAL CHEMISTRY C · NOVEMBER 2013

Impact Factor: 4.77 · DOI: 10.1021/jp409127e

CITATIONS

11

READS

17

2 AUTHORS:



[Jakub D. Baran](#)

University of Bath

17 PUBLICATIONS 177 CITATIONS

SEE PROFILE



[Andreas Larsson](#)

Luleå University of Technology

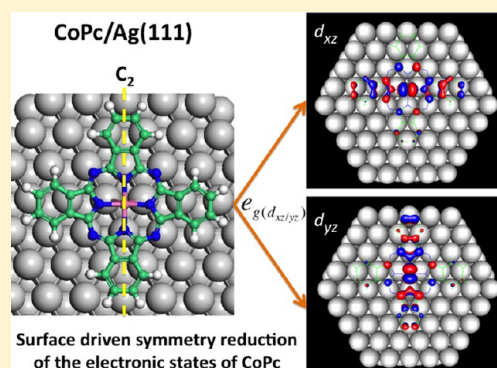
56 PUBLICATIONS 998 CITATIONS

SEE PROFILE

Theoretical Insights into Adsorption of Cobalt Phthalocyanine on Ag(111): A Combination of Chemical and van der Waals Bonding

Jakub D. Baran^{*,†} and J. Andreas Larsson^{†,‡}[†]Tyndall National Institute, University College Cork, Lee Maltings, Prospect Row, Cork, Ireland[‡]Applied Physics, Division of Materials Science, Department of Engineering Sciences and Mathematics, Luleå University of Technology, SE-971 87, Luleå, Sweden

ABSTRACT: In this article we study in detail the interaction of cobalt phthalocyanine (CoPc) with the Ag(111) surface by means of density functional theory calculations (DFT). We discuss the electronic and geometric differences of the adsorbed CoPc as it interacts with the different binding sites of the surface, yielding deeper insight into the adsorption mechanism of organometallic molecules with noble metal surfaces. We interpret the experimentally observed 4-fold to 2-fold symmetry reduction upon interaction of phthalocyanine molecules with metal surfaces as caused by electronic effects originating from nonsymmetric interactions between the molecule and the surface. To assess the role of dispersion forces in bonding of CoPc to the surface we employ a semiempirical dispersion correction to standard DFT and compare the obtained molecule–surface separation with experimental measurements. We show that, in the case of CoPc, the molecule bonds to the surface mostly due to covalent bonding between Co and Ag, but with a considerable contribution from van der Waals bonding between the Pc ligand and the surface. We show in this case where the molecule–surface separation is mostly governed by covalent bonding between the central metal atom and the surface atoms that standard DFT performs reasonably well, as compared to the available experimental data.



I. INTRODUCTION

Metal phthalocyanine (MPc) molecules are of general interest in the field of molecular electronics¹ and catalysis² but also specifically in the study of organic–inorganic interfaces.³ They are commonly used due to the manipulations that can be done utilizing their opto-electronic properties, but also due to their stability (e.g., thermal), which means that they easily form well-ordered assemblies on a variety of surfaces through sublimation. Many transition metal MPc molecules, including cobalt phthalocyanine (CoPc) (see Figure 1), are of great interest since the molecular properties such as the magnetic moment can be easily tuned. The magnetic moment of a MPc can couple to active substrates,^{4,5} which opens the way for a new class of magnetic,^{6,7} and spintronic devices.⁸ MPc molecules containing first row transition metals have also been the subject of a variety of pioneering single molecule imaging, spectroscopy, and manipulation experiments.^{9,10}

MPc molecules have large conformational flexibility,¹¹ which can be triggered as a small but energetic nanomechanical motion, with possible use as molecular switches and memories at the nanoscale.¹² The overlap between the surface and molecular wave functions is of utmost importance for future device designs and their performance, as it determines the charge injection rates and other crucial parameters.¹³ It has been suggested, based on experimental data, that the local charge transfer between the metal surface and the MPc molecule depends on the MPc–surface separation and is site

specific.¹⁴ Because of the unique and complex nature of the MPc–metal surface interaction,¹⁵ a detailed understanding of the physics and chemistry of the interface is essential for optimizing devices based on these materials. Much experimental work has been devoted in recent years to the interaction of different MPc molecules with a variety of metal substrates, in order to deduce the degree of self-assembly, order, and structure of the deposited molecular film. Despite much progress in recent years toward characterization of MPc–metal interfaces, there is still heated discussion concerning the details of the molecular configuration of the MPc with regard to the substrate and the bonding mechanism. In particular, the nature of the MPc–substrate interaction is still elusive, especially regarding the nature of the adsorption, i.e., chemisorption versus physisorption, and the role of the central metal atom and the ligand to the bonding.^{15,16}

At low coverage, individual MPc molecules lie flat and show no tendency to form islands. In general, the adsorption configuration of MPc molecules can be categorized by two parameters: (i) the surface binding site to which the central metal bonds, and (ii) the rotational orientation of the macrocycle with respect to the surface atoms. Although, in principle, the adsorption of MPc molecules could result in a

Received: September 12, 2013

Revised: October 14, 2013

Published: October 16, 2013

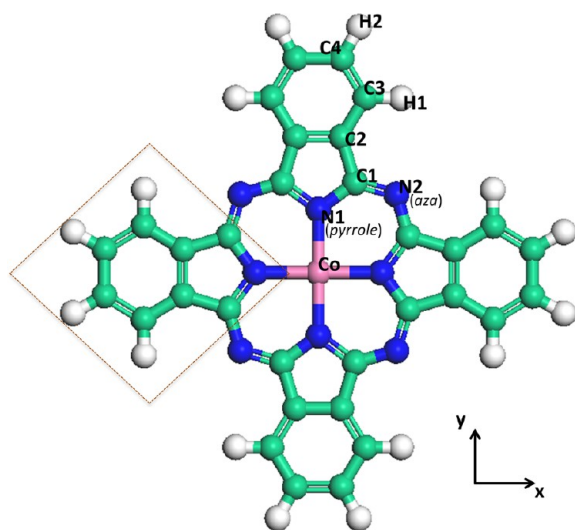


Figure 1. Structure of the CoPc molecule with labeling used in the text. One of the isoindole units is highlighted by a square. There are two isoindole units (macrocycle lobes) pointing along the *y*-axis and two lobes pointing along the *x*-axis, forming perpendicular pairs of lobes.

rich variety of adsorption configurations, only a few have been observed, suggesting a preferential bonding orientation.^{17–24} When thermal energies are very small, the isolated adsorbate is confined to specific adsorption sites and configurations that can be regarded as stable or metastable. These distinct adsorption configurations are stabilized by molecule–surface interactions and can exhibit different electronic and geometric properties. For example, different adsorption configurations change the interaction between the central metal atom associated orbitals and the substrate, which influences the tunneling of electrons through the molecule.²⁵ The adsorption configuration is therefore important for potential molecule device operation and can be probed by scanning tunneling microscopy (STM), which has shown that certain adsorption sites and configurations give rise to a pronounced 4-fold to 2-fold symmetry reduction of the MPc images.^{17,19–21,23,24} In general, STM images of MPc molecules on a metal surface show a “four leaf” pattern (or cross), in accordance with its symmetry in the gas phase. However, in some STM images, the two perpendicular pairs of the Pc ligand lobes (see Figure 1) show a pronounced asymmetry aligned with the close-packed axes of the surface,^{17,19} and one of the directions of the asymmetric cross formed by the Pc ligand appears brighter than the other. This symmetry reduction from 4-fold to 2-fold symmetry upon adsorption could be due to electronic and/or geometric effects. Since STM does not distinguish between these effects, the mechanism of the symmetry reduction still remains elusive.

The aim of this work is to provide deeper understanding of the nature of the interaction between MPc molecules and noble metal surfaces. We analyze the geometric and electronic structure of the planar CoPc molecule on the Ag(111) surface in different adsorption configurations, and the role of different individual orbitals of the free molecule in the bond formation with the surface is discussed. We also propose a possible mechanism behind the 4-fold to 2-fold symmetry reduction of MPc molecules that is sometimes seen in STM upon adsorption. By comparison of the experimentally measured molecule–surface separation with the ground state geometries obtained from standard DFT and DFT-D2, where dispersion

forces are included by means of a semiempirical correction,²⁶ the applicability of these two approaches for studying this and similar systems is evaluated.

II. COMPUTATIONAL METHODS

In this work we perform first-principles calculations using unrestricted DFT with the generalized gradient approximation (GGA) parametrization by Perdew–Burke–Ernzerhof (PBE) for the XC energy,²⁷ and the resolution of the identity (RI) approximation^{28,29} as implemented in the TURBOMOLE v6.1 software package.³⁰ The basis sets are double- ζ split valence augmented by polarization functions, DZVP2, for all atoms. An effective core potential (ECP) was used to take into account scalar relativistic effects: ECP-28-MWB³¹ for Ag.

We have used a cluster representation of the Ag(111) surface to describe the MPc-surface adsorption. Each system under study contains 226 atoms: one CoPc molecule ($\text{CoC}_{32}\text{H}_{16}\text{N}_8$) with 57 atoms and an Ag_{169} cluster with three layers. We used two different conformers of the Ag_{169} cluster, one with an on-top site in the center on one side and a fcc-hollow site in the center of the flip side, and another with a hcp-hollow site in the center on both sides. In addition, the free CoPc molecule was optimized within the same framework. All atoms were allowed to fully relax in the PBE geometry optimizations, with the convergence criteria 10^{-6} Hartree on energy and 10^{-3} Hartree/Bohr for the gradient. Either C_s symmetry or no symmetry was imposed on the system in the calculations.

To account for the missing dispersion effects in the standard implementation of DFT, we describe the van der Waals forces using the semiempirical approach proposed by Grimme²⁶ (DFT-D2 method) in conjunction with the PBE functional. We performed DFT-D2 geometry optimizations starting from the PBE optimized structures with all Ag atoms kept frozen.

Justification of the Used Methodology. Although several DFT based approaches have been used to model the adsorption of porphyrins and phthalocyanines with a central transition metal (M), on various surfaces^{32–35} no consensus has been reached on what approach is most reliable. It has been demonstrated that the calculated electronic configuration of these systems is very sensitive to the choice of DFT functional and basis set.³⁶ Different exchange–correlation (XC) functionals produce different energies and mixing for orbitals with substantial contributions from the M-3d states, including the nature of most chemically significant orbitals of CoPc in the vicinity of Fermi level.³⁶ Some of these properties may not fully be described by any DFT method.³⁷ Marom et al.³⁶ have shown that the density of states (DOS) of molecules calculated by hybrid functionals provides a better fit to the global structure of ultraviolet photoemission spectroscopy (UPS) data, compared to GGA functionals for the free MPc molecule. The inferior performance of GGA functionals was assigned to under-binding of localized orbitals due to self-interaction error.³⁶ The description of the electronic structure of CoPc is also very sensitive to the experimental technique used, and experiment does not bring a definite answer to the nature and energy of the most important CoPc orbitals, as has been shown by Gargiani et al.³⁸ Figure 2 shows the DOS of the free CoPc molecule and the Ag(111) surface calculated with PBE and its hybrid counterpart PBE0.³⁹

Looking at the occupied part of the CoPc spectrum, it can be seen that, although the overall shape of DOS is similar between PBE and PBE0 (see Figure 2a), the PBE0 DOS is downshifted compared to the PBE one. There are also some differences in

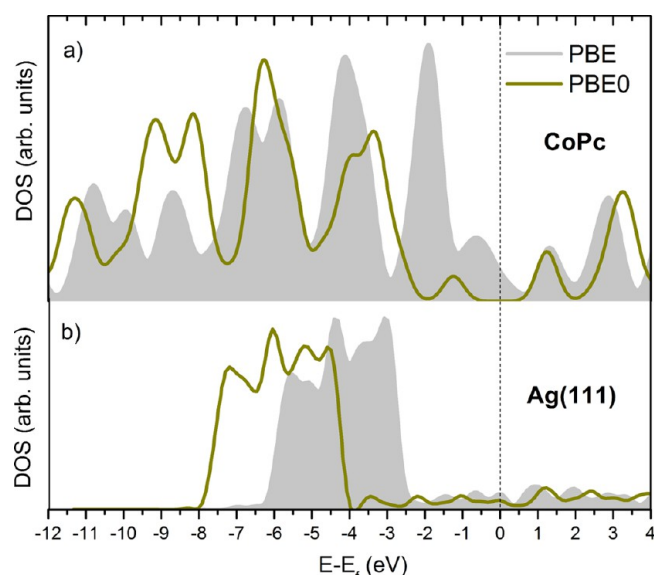


Figure 2. PBE and PBE0 DOS of (a) the free ground state CoPc molecule: spin up and down channels are plotted together; E_f is set in the middle of HOMO–LUMO gap; and (b) the Ag(111) surface. Due to the computational cost of calculating electronic structure of the cluster model of the Ag(111) surface used in this work, we have computed the DOS for a slab model applying the approach described in refs 40–44. Discrete energy levels are broadened with Gaussians of 0.35 eV width for both CoPc and Ag(111).

the height and size of the peaks. The height of the peak around -3.8 eV (PBE0) is decreased and broadened. The use of PBE0 increases the calculated HOMO–LUMO gap from 0.47 to 2.25 eV. As for the unoccupied part of the DOS, minor differences can be seen between PBE and PBE0 (see Figure 2a). For the Ag(111) surface there is downshift of the d-band of Ag(111) (-2.5 to -6.5 eV as for PBE; see Figure 2b). The downshift of the d-band of Ag(111) and DOS of CoPc is caused by the reduced self-interaction within the d-shell due to inclusion of

the Fock-exchange. As shown in Figure 2, this affects the electronic structure of the CoPc and Ag(111) in similar fashion, which suggests that there may be qualitative agreement in the adsorption mechanism for this system predicted by PBE and PBE0. Therefore, although it could be desirable to use hybrid-functionals for description of the CoPc molecule, it is still not yet clear if such calculations applied to the complete CoPc/Ag(111) system would improve its electronic structure, despite bringing an enormous increase in computational cost. This is due to the fact that hybrid functionals that have not been designed to describe the homogeneous electron gas exactly, e.g., B3LYP fails to describe the physics of a metal surface properly,⁴⁵ where GGA functionals perform well.⁴⁶ Therefore, the advantages of hybrid functionals (or any other approach) in the description of the electronic structure of adsorbed transition-metal organic molecules on metallic surfaces can only be properly resolved when such calculations are available, and compared against detailed experimental data revealing unambiguously the position, not only of the crucial occupied levels but also of the unoccupied ones. Since both experimental and theoretical results for MPC–metal surface systems are a field of active research, we use PBE for a balanced description of both the molecule and the metal surface. There are strong indications that this methodology is able to provide a good insight into the electronic structure of this complex system since it: (i) reproduces the CoPc–Ag(111) separation in very good agreement with the experiment.⁴⁷ (ii) Can explain the bias-dependent STM image contrasts⁴⁷ as directly related to the occupancy of the free molecule LUMO, upon adsorption on the surface. (iii) Describes the charge transfer to the LUMO of free CoPc upon adsorption on the Ag(111) surface, in agreement with the recent study of adsorption of CoPc on the Ag(100) surface that has similar work-function to Ag(111),⁴⁸ and which has been validated by hybrid DFT and non-self-consistent GW calculations.⁴⁹

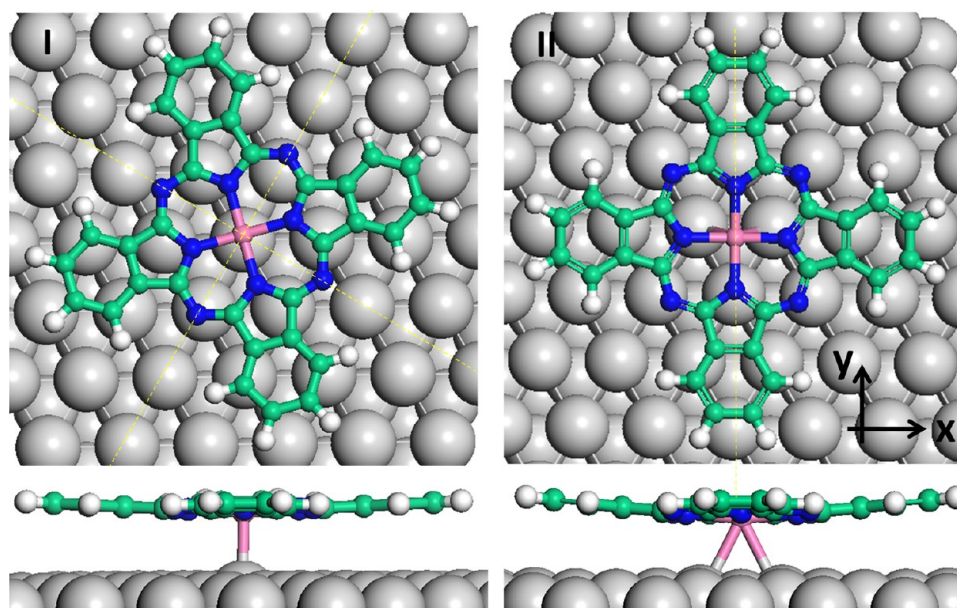


Figure 3. Top and side view of the two stable adsorption configurations of CoPc on Ag(111) resulting from our DFT calculations. The yellow dashes divide the molecule into symmetry equivalent parts with respect to the surface beneath.

Table 1. Central Metal Atom–Ag Surface, and Pc Macrocycle–Ag Surface Distances and Adsorption Energies for CoPc Adsorbed on Ag(111) Resulting from Our Calculations and Experimentally Measured

		DFT	DFT-D2	exp.
configuration I	Co-surface, Å	(2.872 ^a)3.231 ^b	(2.675 ^a)3.054 ^b	2.90(±0.05) ⁴⁷
	Pc-surface, Å	3.4	3.1	-
	<i>E</i> _{ads} , eV	−1.40	−5.89	-
configuration II	Co-surface, Å	(3.053 ^a)3.134 ^b	(2.815 ^a)2.902 ^b	2.90(±0.05)
	Pc-surface, Å	3.3	2.9	-
	<i>E</i> _{ads} , eV	−1.32	−5.85	-

^aBond distance between Co and Ag. ^bDistance between Co and the average Ag position in *z* direction of the first layer, excluding outstanding Ag atoms that are bound to Co.

Table 2. Intramolecular Bond Lengths (in Å) of CoPc in the Gas Phase, and of Configuration I and Configuration II for CoPc Adsorbed on Ag(111) from DFT and DFT-D2 Where the Dispersion Correction Was Included^a

		bond lengths (Å)			
	gas-phase	conf. I		conf. II	
		DFT	DFT-D2	DFT	DFT-D2
Co–N1	1.929	1.921/1.921	1.917/1.916	1.922/1.923	1.918/1.920
N1–C1	1.389	1.392/1.391	1.394/1.390	1.391/1.392	1.392/1.392
C1–N2	1.323	1.324/1.234	1.325/1.324	1.324/1.324	1.325/1.324
C1–C2	1.459	1.459/1.459	1.455/1.455	1.459/1.460	1.455/1.456
C2–C2	1.411	1.413/1.413	1.413/1.413	1.412/1.413	1.414/1.415
C2–C3	1.404	1.405/1.405	1.406/1.406	1.405/1.406	1.405/1.406
C3–C4	1.403	1.406/1.405	1.408/1.409	1.404/1.405	1.406/1.409
C4–C4	1.416	1.416/1.416	1.417/1.417	1.416/1.415	1.416/1.418
C3–H1	1.100	1.100/1.100	1.100/1.100	1.100/1.100	1.100/1.100
C4–H2	1.101	1.101/1.101	1.101/1.101	1.101/1.101	1.101/1.101

^aFor labeling of the atoms, we refer to Figure 1. The two bond length values for the adsorbed molecule correspond to atoms located on the aromatic lobes oriented in two different perpendicular directions with regard to the Ag surface.

III. RESULTS AND DISCUSSION

Experimental studies have found rather disordered CoPc monolayers on Ag(111) with no preferential rotational orientation order.⁴⁷ It is clear from work on other MPc molecules, however, that there is a rich parameter space underpinning the self-assembly of phthalocyanines on metal surfaces.^{17,19} As mentioned above, the configuration of MPc molecules on metal surfaces involves both the position of the central metal atom relative to the atoms of the Ag surface layers (binding site) and the orientation of the molecule relative to the major symmetry axes of the surface (rotational conformation). In order to model the adsorption of CoPc on the Ag(111) surface, we placed the center of the MPc on each of the high-symmetry binding sites of the substrate and performed independent geometry optimizations, allowing all atoms in the system to relax. This resulted in that the CoPc molecule initially placed on the fcc- and hcp-hollow binding site moved either to the on-top or bridge binding adsorption site (see Figure 3). We have consequently found two different binding configurations: configuration I, which has been found to be the most stable, has a binding energy of −1.40 eV, and configuration II, with a binding energy of −1.32 eV (see Table 1). For configuration I, the Co atom is positioned on an on-top binding site, and for configuration II it is adsorbed between the short-bridge and hcp-hollow sites of the surface. Due to the 6-fold symmetry of the Ag(111) substrate, there are three symmetry-equivalent on-top and bridge rotational conformers each. This leads to six different rotational orientations for CoPc on this surface with these two binding configurations. When both these binding configurations are present and the

interactions between the molecules in a monolayer are too weak to be of importance, all six of these rotational directions will be present, which will make the monolayer appear disordered.

In the following, in order to gain better insight into the binding mechanism, and to shed light on the reason for the STM established 4-fold to 2-fold symmetry reduction of some MPc molecules on metal surfaces, we analyze in detail the two adsorption configurations resulting from our calculations (see Figure 3).

In configuration II, the two perpendicular pairs of macrocycle lobes (forming a cross) are aligned along silver atom rows with different packing. That is, one pair of lobes is aligned along one of the closed-packed row of Ag(111) (direction commensurate with the *x*-axis defined here), and the other is aligned with the Ag row perpendicular to it (along the *y*-axis; see Figure 3). For configuration I, the cross is rotated by ~15° compared to configuration II (see Figure 3).

As can be seen from Figure 3, CoPc largely retains its planar character on adsorption with only a small distortion of the aromatic groups, manifested as a slight bending away from the surface. For configuration I the adsorption of CoPc leads to a significant movement of the Ag atom to which the molecule is bonded out of the surface plane (by approximately 0.3 Å). Such a distortion of the substrate silver atoms bonded to MPc and MPor can be explained by charge transfer from the substrate to the molecule and concomitant oxidation of the bonding Ag atom(s).¹⁶ In configuration I, the Co–Ag bond length is 2.872 Å, and the height from the Co to the plane averaged over the Ag atoms of the surface first layer (excluding the protruding Ag atom that bonds to Co) is 3.231 Å (see Table 1).

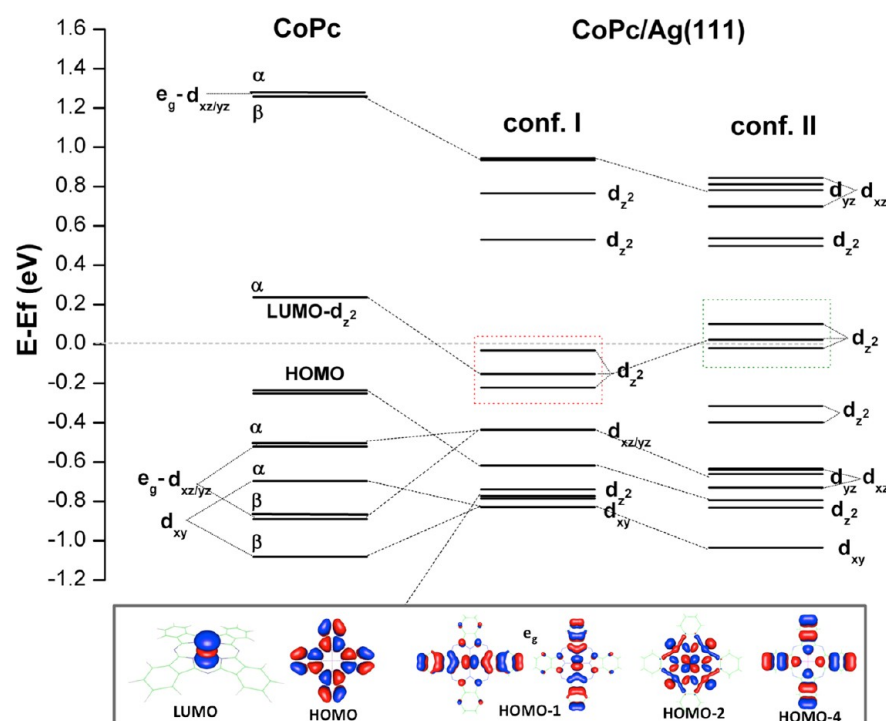


Figure 4. DFT single-particle energy levels of free CoPc (left column), CoPc/Ag(111) – configuration I (center), CoPc/Ag(111) – configuration II (right column). Only energy levels with significant contributions from CoPc are shown. Free CoPc is open-shell, thus both α and β spin orbitals are given. The inset shows some of the frontier orbitals of the free CoPc discussed in the text. The E_f has been chosen in the middle of HOMO–LUMO gap.

In configuration II there is also a similar bending away of the macrocycle from the surface, however, the distortion of the silver atoms that Co is bound to is much smaller (see Figure 3). It is important to notice that in this adsorption configuration, all N atoms lie more or less on top of first layer silver atoms. The bridge binding site has two Co–Ag(111) bond length of 3.053 Å, and a height of the Co from the average position of the first layer Ag of 3.134 Å. Normal Incidence X-ray Standing Wave (NIXSW) measurements of the CoPc monolayer on Ag(111) yield a Co–Ag(111) distance of 2.90 ± 0.05 Å,⁴⁷ in good agreement with the PBE results.

These two adsorption configurations are similar to the adsorption configurations that have been found experimentally and theoretically for several other 3d-transition metal MPc molecules deposited on different coinage metal (111) surfaces.^{17–22} Gao et al.¹⁸ reported adsorption configurations for FePc/Au(111) similar to the ones described here. They found that the adsorption configurations affected the interactions between Fe-*d* orbitals and the substrate, influencing the electron tunneling through the central Fe atom.¹⁸ Change et al.¹⁹ studied by means of STM the adsorption of CoPc, CuPc, and FePc on Cu(111). They observed a 2-fold symmetry reduction of these MPc molecules, which was connected with the adsorption configuration on the surface.¹⁹ These experimental data suggest that the adsorption of MPc molecules on metal substrates can be similar for different metal substrates and different transition metals in the center of MPc, and therefore detailed knowledge of these binding mechanisms is important for progress in the use of these molecules in devices.

To illustrate the geometrical changes of the CoPc molecule upon adsorption on the Ag(111) surface, we compare bond length data for the CoPc molecule in the gas phase to the molecule adsorbed on the Ag(111) surface, listed in Table 2.

Qualitatively, the intramolecular structure of CoPc changes only slightly upon adsorption. This is expected, as additional coordination of the central metal atom in perpendicular direction to the ligand, for this type of molecules, is well-known. However, several subtle changes take place.

One of the most interesting features of the bond length data presented in Table 2 is the change of the Co–N1 bond length upon adsorption. The Co–N1 bond length for the free CoPc is 1.929 Å. Upon adsorption the Co–N1 bond is slightly shortened for both the adsorption configurations. On the other hand, the bonds of the benzene carbons are slightly elongated. We discuss an interrelation of the geometrical changes and the electronic structure in the following sections.

In our calculations of CoPc adsorption on Ag(111), the symmetry of the molecule is largely preserved (see Table 2). In fact, the largest deviations from C_{4v} concern the Co–N bonds. All other bond lengths on the two different pairs of perpendicular aromatic lobes differ by only 0.001 Å (0.002 Å for DFT-D2; see Table 2). Also, for neither configuration I nor II are there any noticeable differences in the height of the different isoindole units from the Ag(111) surface. It is clear that the geometrical changes of the molecule caused by the bonding to the surface cannot explain the 2-fold symmetry reduction observed in STM, but electronic effects also need to be investigated to deduce the symmetry reduction seen in STM.

The differences in binding mechanism between configuration I and II can be understood from an in-depth examination of the evolution of the electronic states upon adsorption of the molecule on the surface within the limits of the DFT method chosen. In Figure 4, we present single-particle levels of the isolated and the adsorbed CoPc molecule in configuration I and II.

Before discussing the adsorption effect on the electronic structure of the CoPc molecule we present the electronic configuration of the gas-phase molecule. In the free CoPc molecule (D_{4h} symmetry), the 3d orbitals are split into three nondegenerate levels, with d_{z^2} (a_{1g}), $d_{x^2-y^2}$ (b_{1g}) and d_{xy} (b_{2g}) (clearly detected in photoemission spectra)³⁸ symmetries and a degenerate pair $d_{xz/yz}$ (e_g). All of these are occupied except $d_{x^2-y^2}$, which is completely empty, and d_{z^2} which is single occupied giving this molecule a magnetic moment. The relative position of the a_{1g} and e_g states with Co character is controversial, because the latter are not unambiguously detected in photoemission spectra,^{49,50} and the DFT predictions are affected by the use of different XC-functionals,^{34,51,52} e.g., hybrid functionals³⁶ as well as DFT+U⁵² reverses the position of the unoccupied a_{1g} and e_g states compared to the order obtained with GGA functionals, where these are LUMO and LUMO+1, respectively. The question of the true position of these unoccupied molecular levels, however, will be only fully explained when the corresponding experimental spectrum is obtained.

The first column in Figure 4 displays the calculated energy spectrum of free CoPc in the vicinity of the Fermi level as resulting from PBE. According to our calculations, the HOMO is of a_{1u} symmetry and entirely located on the macrocycle carbons. The LUMO (a_{1g}) has purely d_{z^2} character and the LUMO+1 and HOMO-1 orbitals are doubly degenerate e_g orbitals with both Co-3d_{xz/yz} and macrocycle character (see inset to Figure 4). The occupied counterpart to LUMO (a_{1g}) is below the energy range shown in Figure 4 at -2.3 eV.

According to our calculations, the difference between spin-up and spin-down channels disappear upon adsorption of CoPc, showing that the magnetic moment of the free molecule has been quenched.⁵³ Looking first at the most stable adsorption configuration resulting from our calculations (configuration I), we discern that the free molecule LUMO, which has Co-3d_{z²} character, has been lowered below the Fermi level (E_f) and is distributed among, and mixed with Ag orbitals that result in a few orbitals with bonding and antibonding character below and above the E_f . The shifting below the E_f of Ag(111) means that LUMO has been populated by charge density from the surface which is in line with the experimental studies^{49,53,54} and DFT+U calculations.⁵² The mixing of the Co orbitals and charge density transfer into the LUMO is indicative of chemical bonding between Co and the surface, and we find that the Co-3d_{z²} orbital interacts with the entire *sp* band of Ag. The molecule also binds to the surface with a substantial adsorption energy (1.32–1.40 eV). The occupation of the LUMO is of prime importance both for the structural properties and for the features of the STM images of the system.⁵⁵ Such population of the LUMO has been observed in XPS and UPS measurements for other cobalt porphyrins and phthalocyanines.^{32,53,54} Thus, DFT captures the most striking features of these systems. There is also a significant downshift of the other CoPc MOs in the CoPc/Ag(111) complex, indicative of strong charge redistribution in the CoPc molecule upon adsorption. Due to the above-mentioned difficulties in describing the relative position of the *d*-levels, which differ using different XC-functionals, it cannot be excluded that use of other XC-functionals may affect the calculated molecule–surface charge-transfer.

Turning to configuration II, we find that there are three states with Co-3d_{z²} character at and above the Fermi level, which are all below the Fermi level in configuration I, as

indicated by dashed squares in Figure 4. These states are derived from the free CoPc LUMO, thus this orbital is slightly less occupied in configuration II than in configuration I. This is seen in Figure 5, which shows a comparison of the partial density of states (PDOS) of the Co-3d states for these two adsorption configurations.

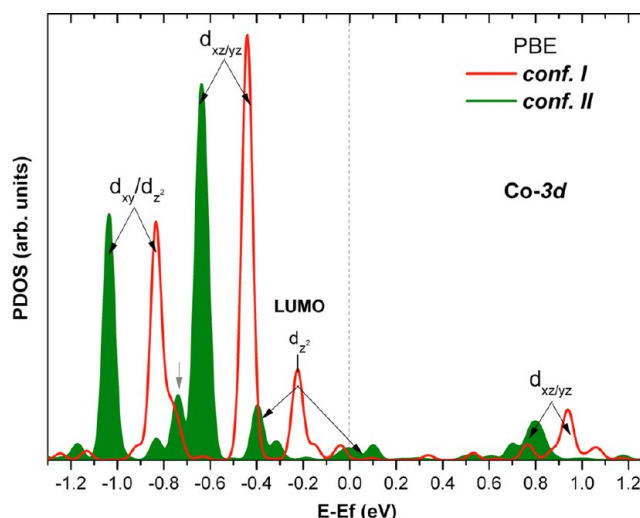


Figure 5. PDOS of the Co-3d states of CoPc/Ag(111) for configuration I and configuration II obtained from the PBE calculations.

As mentioned above, the peak corresponding to the former LUMO of Co-3d_{z²} character is entirely shifted below the Fermi level in configuration I (see Figure 5). However, in configuration II we find that the height of this peak is reduced (see peak around -0.40 eV) and that there are some states just above the Fermi level. The peak corresponding to Co-3d_{xz/yz} states at -0.45 eV in configuration I, has been shifted to -0.65 eV and broadened in configuration II. There are also additional small peaks next to it, showing a splitting of the d_{xz} and d_{yz} states. This is also the case for the Co-3d_{xy} peak and the Co-3d_{xz/yz} above the E_f (see Figure 5). Since some of the binding energy of the CoPc molecule on Ag(111) is due to bonding through the CoPc LUMO, the adsorption on the “near-bridge” site (configuration II) is slightly less energetically favorable (80 meV) because it results in a smaller population of the 3d_{z²} orbital. We explain this as follows: when the CoPc molecule is adsorbed in configuration I, Co is directly bonded to a single Ag atom of the surface, resulting in a greater overlap of this orbital with the surface states and therefore a larger charge transfer to Co, than when adsorbed on the bridge site. This contributes to a higher adsorption energy and shorter Co–Ag bond length for configuration I.

Another important difference seen in Figure 4 between configuration I and configuration II concerns the position of the Co-3d_{xz/yz} states. In configuration II, Co is positioned almost in the center between Ag atoms of a short- and long-bridge (see Figure 3). In this configuration, Co coordinates with four Ag atoms: two of the short-bridge with a distance of 3.282 Å and two at the long-bridge with slightly longer distances of 4.232 and 3.744 Å. Due to the symmetry of the Co environment in configuration II, the Co-3d_{xz/yz} orbitals are optimally directed toward the short-bridge and long-bridge Ag atoms, which leads to better overlap of these states with the Ag-4d_{xz/yz} than for configuration I. This results in a further

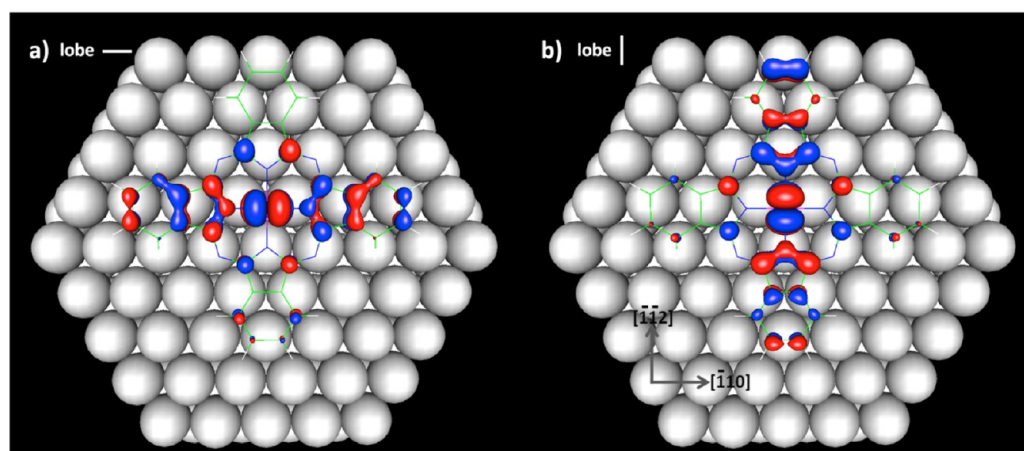


Figure 6. Two nondegenerate molecular orbitals of configuration II originating from the split of the double degenerate HOMO-1 of e_g symmetry of the free molecule upon adsorption of the CoPc on the Ag(111). (a) The state at -0.72 eV, with the Co and the isoindole units aligned with one of the closed-packed rows of Ag atoms of the substrate. (b) The state at -0.66 eV, with the Co and the isoindole units aligned with one of the rows perpendicular to the closed-packed ones. Plots were made with the value of isosurface of ± 0.01 e/ \AA^3 .

downshift of the Co- $3d_{xz/yz}$ states for configuration II (see Figure 5). These are also split, which means that the degeneracy of the $3d_{xz/yz}$ states (these are orbitals of e_g symmetry e.g. HOMO-1 and LUMO+1 in the free molecule) is lifted for this adsorption configuration. Addition of dispersion forces results in shift of around 0.2 eV toward lower binding energies. Figure 6 shows the two nondegenerate states at -0.72 and -0.66 eV resulting from splitting of the HOMO-1 of CoPc molecule for configuration II. The splitting of the Co- $3d_{xz/yz}$ states is also present for the on-top binding site; however, it is too small to be of importance.

Since the doubly degenerate e_g orbitals have mixed Co- $3d_{xz/yz}$ and ligand character (see inset to Figure 4), the pairs of perpendicular molecular lobes also interact with the surface differently along the close-packed (lobe $-$) and the less close-packed (lobe $|$) rows (see Figure 6). Note that no on-top configuration with the Pc macrocycle lobes aligned as in configuration II has been obtained in our DFT calculations. A geometry optimization starting from such a structure resulted in configuration II, i.e., the molecule moved along the $[1\bar{1}2]$ direction of the surface.

The uneven interaction of the Co- $3d_{xz/yz}$ states with the Ag atoms at the bridge binding site, as well as the interaction of the Pc lobes with the silver atom rows of different packing lifts the degeneracy of the free CoPc e_g orbitals. The increased overlap of the Co- $3d_{xz/yz}$ with the surface states is counteracted by a reduced overlap of the Co- $3d_{z^2}$ orbital with the substrate, which results in a slightly lower binding energy in the near-bridge site compared to the on-top binding site. It is the incompatibility of the molecular and surface symmetries that results in different atomic configurations beneath the two perpendicular molecular axes. As a consequence, the strength of the molecule–surface interactions is not uniform along these perpendicular surface directions, and, thus, the symmetry of the molecule is broken and the e_g ($d_{xz/yz}$) states split. The Natural Bond Orbital (NBO) charges also show that for configuration II there is a small 0.1e (0.2e for DFT-D2) difference in charge transfer between the lobe $-$ and lobe $|$.

For configuration I, the above-mentioned splitting of the double degenerate e_g CoPc orbitals with Co- $3d_{xz/yz}$ contribution is virtually nonexistent (see Figure 4). In this configuration the molecule buckles more, with the Co ion being pulled out of

the macrocycle plane toward the substrate due to the strong interaction of Co with the silver surface, but the molecule approximately preserving its 4-fold symmetric structure (C_{4v}). The near-degeneracy of the states with Co- $3d_{xz/yz}$ contribution is directly connected to the orientation of the CoPc molecule with respect to the symmetry of the Ag(111) surface. The contrasting symmetry features of the two adsorption configurations can be clearly seen comparing the lines showing coinciding mirror planes of the molecule and the surface in Figure 3. As can be seen in Figure 3, all the pyrrole nitrogens (and whole isoindole units) are in equivalent positions with respect to the surface atoms in configuration I. It is only the aza nitrogens that are in nonequivalent positions with respect to the surface. This leads to the almost uniform interaction of the Co- $3d_{xz/yz}$ and N-pyrrole $2p_z$ states and the Ag atoms for each isoindole unit in configuration I.

Chang et al.¹⁹ observed a 4-fold to 2-fold symmetry reduction of CoPc on Cu(111) as long as contributions of the d_{z^2} states to the tunneling process did not become dominant. On the Cu substrate they only observed one bonding configuration, with three orientations with one of the Pc lobe pairs pointing in the direction of the close-packed Cu atom rows, corresponding to our configuration II on Ag(111). We explain this effect by the fact that when the molecules adsorb in conf. II, double degenerate e_g orbitals, i.e., HOMO-1 and LUMO+1 that are localized on the perpendicular aromatic lobes, are split into a new set of orbitals with different energies that give rise to different balance of electron tunneling from these states, which result in the observed symmetry reduction seen in STM images.⁵⁶ It is interesting to note that we do not observe any split in these orbitals for configuration I, where the $3d_{z^2}$ orbital has an optimal overlap with the underlying on-top metal atom. Future experiments and/or simulations are needed to determine whether the reverting back to 4-fold symmetry that they observe when tunneling through d_{z^2} states is connected with a change in binding site (near-bridge to on-top) and Pc-ligand orientation (ca. 15° rotation), or if the filling of the d_{z^2} orbital of Co is intrinsically linked to the splitting of the $3d_{xz/yz}$ orbitals. In addition, the molecule–substrate charge transfer is slightly different for perpendicular macrocycle lobe pairs, which can influence the STM images as well, as has been postulated by Wang et al.¹⁷ However, our analysis of the CoPc

geometry and charge for configuration II indicates only minor differences between perpendicular CoPc lobes, i.e., the effect is an electronic 2-fold symmetry reduction, which affects the energy levels and tunneling properties of the molecule,⁵² not its geometry as has been suggested for CoPc adsorption on the Cu(111) surface.⁵⁷

Figure 7 shows the PDOS of the pyrrole N-2p states for the free and surface bound CoPc, which is practically identical for configurations I and II.

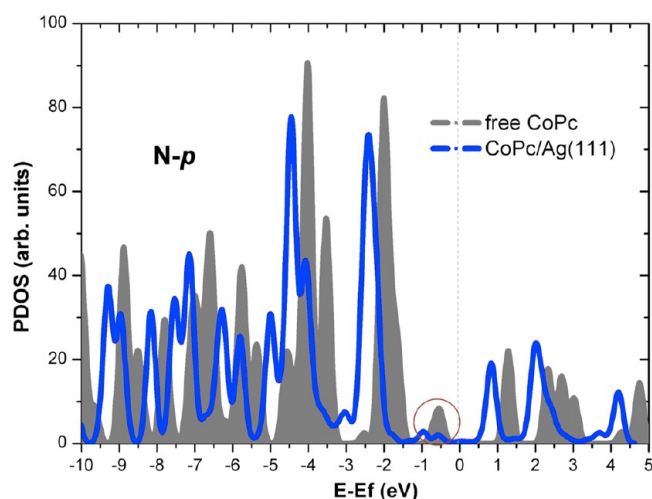


Figure 7. PDOS of pyrrole nitrogen 2p states for the free (gray) and surface bound in conf. II (blue). Red circle highlights N-states connected with a charge transfer to the surface.

After adsorption, the N-p peaks of the free CoPc around -0.5 eV disappear, and the other peaks are shifted to lower energies by ca. 0.3 eV. Such a downshift of the PDOS suggests that N-p orbitals also play a role in the hybridization with the surface and there may be a charge transfer from the nitrogens to the surface as has been postulated by Bai et al.⁵⁸ for cobalt(II) octaethylporphyrin on Ag(111), based on X-ray photoelectron spectroscopy (XPS) measurements. Another explanation of these phenomena is that they result from rearrangement of the electron density on the pyrrole nitrogens, caused by the charge transfer between Co and the surface. That is, additional charge density on the Co atom may cause a change of the electron density of the neighboring pyrrole nitrogens.

Further insight into the bonding mechanism of the CoPc on Ag(111) can be gained if one considers the interactions of the isoindole units with the surface. As mentioned above, the charge analysis reveals only a slight difference in charge between perpendicular aromatic lobes of the adsorbed molecule. Figure 8 shows the PDOS of the carbon 2p states for these perpendicular aromatic lobes for configuration I and II compared to the free molecule. On close inspection one can see that there are subtle differences for the e_g states (peaks corresponding to former HOMO-1 and LUMO+1) that are mostly localized on the perpendicular aromatic lobes with substantial contribution of the Co- $3d_{xz/yz}$ states as shown in the inset to Figure 4.

In general, the C-2p peaks are shifted toward lower energies for both configuration I and II upon adsorption of the CoPc molecule on Ag(111), with the shift for the latter being slightly larger. There is a reduction of the size of peaks in the region

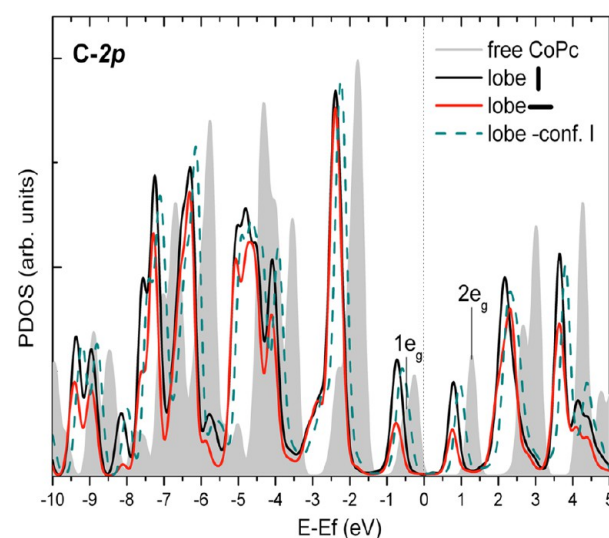


Figure 8. PDOS of the C-2p states for the perpendicular lobes of CoPc for configuration II obtained from PBE. Only PDOS for one lobe for the free molecule and configuration I is shown due to their symmetry equivalence/near symmetry equivalence, respectively. Peaks corresponding to the e_g states closest to the Fermi level are indicated. For labeling of the lobes, see Figure 1 and Figure 3

between -3.5 and -5.5 eV that reflects the coupling of the states localized on the Pc with the surface d -band. The most interesting feature emerging from Figure 8 is comparing the C-2p PDOS between two perpendicular lobes for these two configurations. The peaks that correspond to the formerly degenerate states of the free molecule (see features around ± 0.8 eV of the Fermi level in Figure 3) for the lobe $-$ are almost half the size of the peaks for the lobe I . Note that the size of the peaks for the lobe I is almost the same as for configuration I for which no difference between perpendicular lobes was found. The different population of the states localized on lobes pointing in different perpendicular directions is due to their interaction with the silver rows with different packing and the Co atom's different interactions concerning $3d_{xz}$ and $3d_{yz}$ with the surface atoms. This breaks the symmetry of the doubly degenerate $1e_g$ and $2e_g$ orbitals localized on the macrocycle and as a consequence the molecular density lowers its 4-fold rotational symmetry to 2-fold, which can be seen when the electron population changes as result of the STM modulation. According to our calculations, the charge transfer between the molecule and the surface mostly involves the aromatic carbon atoms and the charge difference between the perpendicular set of isoindole units could appear in STM images as different brightness of the perpendicular lobes. Heinrich et al.²⁵ demonstrated for CoPc on the Cu(111) surface that, apart from the tunneling channels localized on the Co atom, there are also other conduction channels located on the isoindole legs. They found that the conduction from these channels play a prominent role in the molecular conductance of CoPc, and is responsible for the symmetry changes of CoPc,²⁵ supporting our results.

We expect this effect to be more pronounced for first-row transition metal MPc molecules with further filled d states (NiPc, CuPc, and ZnPc) than for CoPc, because the LUMO of these molecules is e_g symmetric, which in the case of the charge transfer to this orbital would result in the molecule being susceptible to a Jahn–Teller-like distortion.^{38,59} Due to the difficulties noted in the Computational Method section in

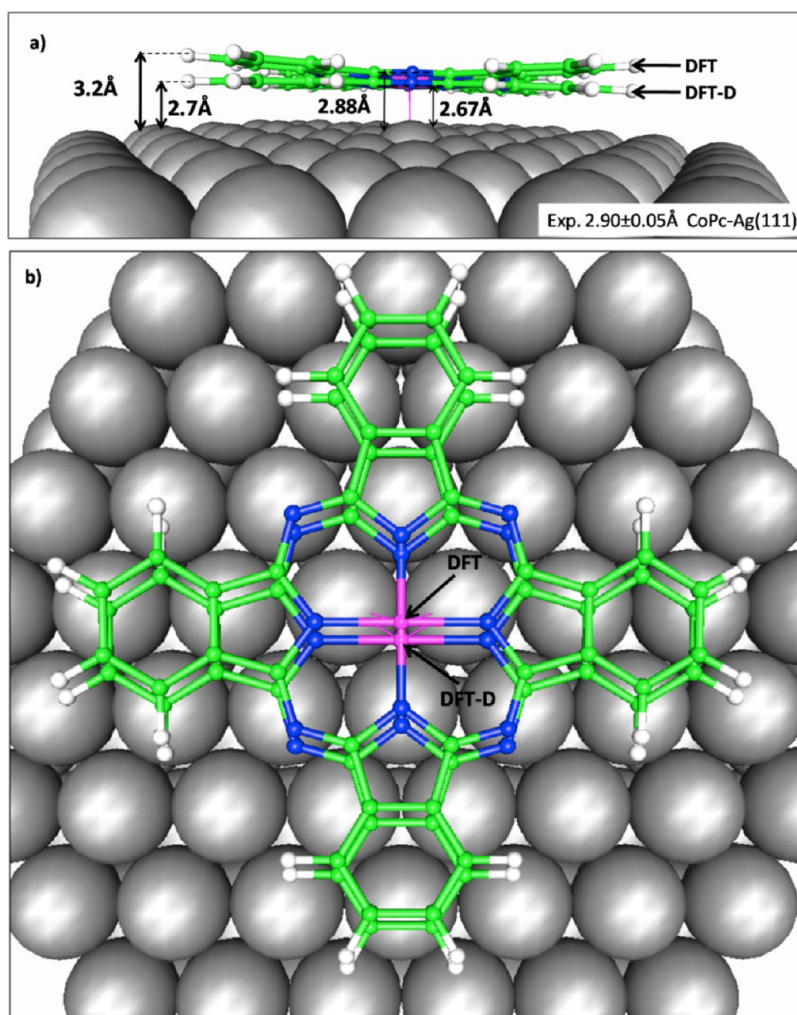


Figure 9. Superimposed CoPc/Ag(111) structures resulted from DFT and DFT-D2 calculations: (a) side view of configuration I; (b) top view of configuration II.

describing the relative sequence of the frontier orbitals with the metal 3d character in MPc molecules by DFT, we cannot exclude that in reality there is also partial occupation of the unoccupied $2e_g$ states (LUMO+1 in free CoPc, see Figure 4) upon adsorption.

The magnitude of the MPc - substrate charge transfer and splitting of the $M-3d_{xz/yz}$ states should vary for different MPc/surface systems. The population of the CoPc unoccupied orbitals by electrons from the surface is in line with work of Gargiani et al.³⁸ where it has been shown, that indeed, the electron injection process of MPc molecules depends on the degeneracy and on the symmetry of the actual molecular states available for electron localization. They have found that thin films of MPc molecules with almost filled d states (NiPc, CuPc, ZnPc) behave identically upon potassium doping, where the injected electrons filled the LUMO localized on the macrocycle with e_g symmetry that host up to four electrons per molecule at K saturation. However, they found that in the case of CoPc, the electron filling process involves first the empty states localized on Co (a_{1g}/e_g symmetric orbitals) with the remaining electrons being transferred to the higher lying e_g orbitals resulting in a total of 5–6 electrons per molecule at complete potassium intercalation.³⁸ This would be in line with the electronic structure of the free CoPc obtained from our calculations and can be attributed to the filling of LUMO of a_{1g} symmetry and

further the LUMO+1 of e_g symmetry upon adsorption on the surface.

IV. VAN DER WAALS FORCES

In the following we investigate in detail the difference in the interaction of the extended π -system of the Pc ligand with the surface states when using DFT-D.

It has been reported that molecules like 3,4,9,10-perylene-tetracarboxylic acid dianhydride (PTCDA), with an extended π -system but without a central metal atom and other distinct reactive center, lock in specific adsorption sites on the Ag(111) surface, driven by the molecular π -system–substrate interaction.⁶⁰ This is of weak van der Waals-type (vdW), and can be ascribed to the coupling between the electrostatic moments of the molecule and the substrate, including induced moments. Since this is a collective phenomenon extending over many atoms, such interactions are usually less dependent on the actual adsorption site of the molecule. The term “vdW forces” can refer to different types of intermolecular interactions, such as electrostatics (between permanent multipoles), induction (permanent multipole-induced multipole interactions), and dispersion (induced multipole-induced multipole interaction). Experimental estimates of the binding energies of vdW bound molecules on metal surfaces are scarce, but it has been reported

that azobenzene physisorbs on Ag(111) with a binding energy of ~ 1.08 eV.⁶¹ It seems plausible that the contribution from vdW bonding for CoPc (57 atoms) would match, or even exceed the binding energy of azobenzene (24 atoms). Our simulations using PBE obtains a CoPc-Ag(111) binding energy of ~ 1.4 eV, where the main contribution is from Co–Ag chemisorption, since it is known that the commonly used DFT functionals fail to capture dispersion effects that are extremely important to describe molecule–substrate interactions that are governed by vdW forces (physisorption). The CoPc molecule primarily bonds to the surface through the Co atom, which is captured well by the PBE method used here; however, the binding energies seems to be underestimated for CoPc as we previously also have reported for SnPc.⁵⁶ The interactions through the ligand are of vdW nature and therefore not described well with PBE. Therefore, other methods have to be sought to describe the Pc–substrate interaction. Table 1 lists the adsorption energies and the molecule–surface distances that resulted from DFT-D2.

When the dispersion correction is switched on, the molecule flattens and moves closer to the surface (see Figure 9a). The Co–surface distance decreases by 0.197 and 0.238 Å, while the adsorption energy increases by 4.47 and 4.63 eV, for configuration I and configuration II, respectively (see Table 1). The molecular position on the adsorption site is almost not affected by dispersion effects in configuration I; however, for configuration II the molecule shifts toward the hcp-hollow site (see Figure 9b).

This can be explained by the orbital interactions as the molecule is pushed closer toward the surface in DFT-D2. The shift toward the underlying silver atom of the second layer at the hcp-hollow site leads to better overlap of the Co- d_{z^2} with the surface states.

Geometry optimization with DFT-D2 for configuration I results in a Co–Ag(111) separation of 3.054 Å from the average position of all Ag atoms excluding the outstanding Ag atom to which Co is bound to (Co–Ag bond length of 2.675 Å, see Table 1). Comparison with the experimental distance of $2.90(\pm 0.05)$ Å, and the PBE value of 3.231 Å (Co–Ag bond length of 2.872 Å), indicates that standard DFT (PBE) models the adsorption geometry of CoPc on Ag(111) reasonably well, despite that neglects of vdW/dispersion effects. In addition, the dispersion correction to the binding energy predicted by DFT-D2 is most probably grossly overestimated, as has also been found in other studies.^{61,62} Therefore, we can expect the adsorption energy to lie somewhere between the underestimated ~ 1.4 eV predicted by DFT and the overestimated ~ 5.9 eV predicted by DFT-D2. Nevertheless, the dispersion correction is useful because it shows that the vdW forces make significant contributions to the bonding in these type of systems, and are needed to obtain geometries that are in quantitative agreement with experiment.

V. CONCLUSIONS

We have found two favorable bonding configurations of CoPc on Ag(111): on the on-top and the near-bridge binding sites. By comparison of the electronic structure and geometry of the two different adsorption configurations, we get deeper insight into the mechanism of bonding and shed light on the origin of the 4-fold to 2-fold symmetry reduction observed in STM of MPc molecules on metal surfaces. We found that the orientation of the CoPc molecule on the Ag(111) surface strongly correlates with the crystallographic axes of the surface

and that there are subtle but important differences in the geometric and electronic structure for the two binding sites that our simulations find favorably bond CoPc. We find that adsorption of the CoPc on Ag(111) is site specific and driven by a delicate balance between contributions from Co- $3d_{z^2}$ and Co- $3d_{xz/yz}$ and even N-p states, as well as by weak interactions of the aromatic lobes and the underlying rows of surface atoms along different crystallographic direction. Our calculations show that the mechanism behind the reputed 2-fold symmetric STM images of MPc molecules on noble metal surfaces is surface driven, and is attributed to electronic, rather than geometric effects. Our suggested mechanism for the symmetry reduction of the CoPc from 4-fold to 2-fold distinguishes between the adsorption configuration when the perpendicular pairs of ligand lobes are aligned with the silver atom rows (near-bridge) and not (on-top), in agreement with experiment. The interaction of the macrocycle lobes along these silver rows only results in slightly different charge transfer between these perpendicular aromatic lobes and the surface. However, we find that for this specific adsorption configuration, the degeneracy of the e_g symmetric orbitals, e.g., HOMO-1 and LUMO+1, which have mixed Co- $3d_{xz/yz}$ and ligand character, is lifted, resulting in a new set of orbitals that are not equally populated by electrons from the surface.

Dispersion correction within the DFT-D2 scheme improves the agreement with experiment for the molecule–surface separation to be quantitative. However, it suggests an increase of the binding energy by inclusion of van der Waals-like forces that is so substantial it is more likely to be overestimated within the approach used in this work. To better assess the contribution of the vdW forces to the binding energy, other correlated methods are needed but are presently computationally unfeasible for a system of this size.

In this work we provide understanding of the binding mechanism of transition metal-phthalocyanine molecules with metal surfaces that should be beneficial for the construction of future experiments and devices based on these molecules.

■ AUTHOR INFORMATION

Corresponding Author

*Mailing address: Competence Centre for Catalysis and Department of Applied Physics Chalmers University of Technology, SE-412 96, Göteborg, Sweden. E-mail: jakub.baran@chalmers.se.

Notes

The authors declare no competing financial interest.

■ ACKNOWLEDGMENTS

This work was supported by the Science Foundation Ireland and the FP6Marie Curie Early Stage Training Network NANOCAGE (MEST-CT-2004-506854). The authors wish to acknowledge the SFI/HEA Irish Centre for High End Computing (ICHEC) for the provision of computational facilities, and SFI/HEA for the provision of local computing clusters. We also thank S. D. Elliott and P. J. Moriarty for reading the manuscript and providing useful comments.

■ REFERENCES

- (1) Forrest, S. R. The Path to Ubiquitous and Low-Cost Organic Electronic Appliances on Plastic. *Nature* **2004**, *428* (6986), 911–918.
- (2) Raymond, J. A New Fuel Cell Cathode Catalyst. *Nature* **1964**, *201*, 1212–1213.

- (3) Stadler, C.; Hansen, S.; Kroger, I.; Kumpf, C.; Umbach, E. Tuning Intermolecular Interaction in Long-Range-Ordered Submonolayer Organic Films. *Nat. Phys.* **2009**, *5* (2), 153–158.
- (4) Iacovita, C.; Rastei, M. V.; Heinrich, B. W.; Brumme, T.; Kortus, J.; Limot, L.; Bucher, J. P. Visualizing the Spin of Individual Cobalt-Phthalocyanine Molecules. *Phys. Rev. Lett.* **2008**, *101* (11), 4.
- (5) Basiuk, E. V.; Basiuk, V. A.; Santiago, P.; Puente-Lee, I. Noncovalent Functionalization of Carbon Nanotubes With porphyrins: Meso-tetraphenylporphyrin and Its Transition Metal Complexes. *J. Nanosci. Nanotechnol.* **2007**, *7* (4–5), 1530–1538.
- (6) Zhao, A. D.; Li, Q. X.; Chen, L.; Xiang, H. J.; Wang, W. H.; Pan, S.; Wang, B.; Xiao, X. D.; Yang, J. L.; Hou, J. G.; Zhu, Q. S. Controlling the Kondo Effect of an Adsorbed Magnetic Ion through Its Chemical Bonding. *Science* **2005**, *309* (5740), 1542–1544.
- (7) Wende, H.; Bernien, M.; Luo, J.; Sorg, C.; Ponpandian, N.; Kurde, J.; Miguel, J.; Piantek, M.; Xu, X.; Eckhold, P.; Kuch, W.; Baberschke, K.; Panchmatia, P. M.; Sanyal, B.; Oppeneer, P. M.; Eriksson, O. Substrate-Induced Magnetic Ordering and Switching of Iron Porphyrin Molecules. *Nat. Mater.* **2007**, *6* (7), 516–520.
- (8) Rocha, A. R.; Garcia-Suarez, V. M.; Bailey, S. W.; Lambert, C. J.; Ferrer, J.; Sanvito, S. Towards Molecular Spintronics. *Nat. Mater.* **2005**, *4* (4), 335–339.
- (9) Lippel, P. H.; Wilson, R. J.; Miller, M. D.; Wöll, C.; Chiang, S. High-Resolution Imaging of Copper-Phthalocyanine by Scanning-Tunneling Microscopy. *Phys. Rev. Lett.* **1989**, *62* (2), 171.
- (10) Gimzewski, J. K.; Stoll, E.; Schlittler, R. R. Scanning Tunneling Microscopy of Individual Molecules of Copper Phthalocyanine Adsorbed on Polycrystalline Silver Surfaces. *Surf. Sci.* **1987**, *181* (1–2), 267–277.
- (11) Baran, J. D.; Larsson, J. A. Inversion of the Shuttlecock Shaped Metal Phthalocyanines MPc (M = Ge, Sn, Pb)—A Density Functional Study. *Phys. Chem. Chem. Phys.* **2010**, *12* (23), 6179–6186.
- (12) Tao, N. J. Molecular Switches: Pushing the Right Button. *Nat. Chem.* **2009**, *1* (2), 108–109.
- (13) Hwang, J.; Wan, A.; Kahn, A. Energetics of Metal-Organic Interfaces: New Experiments and Assessment of the Field. *Mater. Sci. Eng.: R. Rep.* **2009**, *64*, 1–31.
- (14) Peisert, H.; Kolacyak, D.; Chasse, T. Site-Specific Charge-Transfer Screening at Organic/Metal Interfaces. *J. Phys. Chem. C* **2009**, *113* (44), 19244–19250.
- (15) Lindner, S.; Treske, U.; Knupfer, M. The Complex Nature of Phthalocyanine/Gold Interfaces. *App. Surf. Sci.* **2013**, *267*, 62–65.
- (16) Gottfried, J. M.; Marbach, H. Surface-Confined Coordination Chemistry with Porphyrins and Phthalocyanines: Aspects of Formation, Electronic Structure, and Reactivity. *Z. Phys. Chem.: Int. J. Res. Phys. Chem. Chem. Phys.* **2009**, *223* (1–2), 53–74.
- (17) Wang, Y. F.; Ge, X.; Manzano, C.; Korger, J.; Berndt, R.; Hofer, W. A.; Tang, H.; Cerda, J. Supramolecular Patterns Controlled by Electron Interference and Direct Intermolecular Interactions. *J. Am. Chem. Soc.* **2009**, *131* (30), 10400–10402.
- (18) Gao, L.; Ji, W.; Hu, Y. B.; Cheng, Z. H.; Deng, Z. T.; Liu, Q.; Jiang, N.; Lin, X.; Guo, W.; Du, S. X.; Hofer, W. A.; Xie, X. C.; Gao, H. J. Site-Specific Kondo Effect at Ambient Temperatures in Iron-Based Molecules. *Phys. Rev. Lett.* **2007**, *99* (10), 106402.
- (19) Chang, S.-H.; Kuck, S.; Brede, J.; Lichtenstein, L.; Hoffmann, G.; Wiesendanger, R. Symmetry Reduction of Metal Phthalocyanines on Metals. *Phys. Rev. B* **2008**, *78* (23), 233409.
- (20) Manandhar, K.; Park, K. T.; Ma, S.; Hrbek, J. Heteroepitaxial Thin Film of Iron Phthalocyanine on Ag(111). *Surf. Sci.* **2009**, *603* (4), 636–640.
- (21) Karacuban, H.; Lange, M.; Schaffert, J.; Weingart, O.; Wagner, T.; Möller, R. Substrate-Induced Symmetry Reduction of CuPc on Cu(1 1 1): An LT-STM Study. *Surf. Sci.* **2009**, *603* (5), L39–L43.
- (22) Jiang, P.; Ma, X. C.; Ning, Y. X.; Song, C. L.; Chen, X.; Jia, J. F.; Xue, Q. K. Quantum Size Effect Directed Selective Self-Assembling of Cobalt Phthalocyanine on Pb(111) Thin Films. *J. Am. Chem. Soc.* **2008**, *130* (25), 7790–7791.
- (23) Nazin, G. V.; Qiu, X. H.; Ho, W. Visualization and Spectroscopy of a Metal–Molecule–Metal Bridge. *Science* **2003**, *302* (5642), 77–81.
- (24) Qiu, X. H.; Nazin, G. V.; Ho, W. Vibronic States in Single Molecule Electron Transport. *Phys. Rev. Lett.* **2004**, *92* (20), 206102.
- (25) Heinrich, B. W.; Iacovita, C.; Brumme, T.; Choi, D.-J.; Limot, L.; Rastei, M. V.; Hofer, W. A.; Kortus, J.; Bucher, J.-P. Direct Observation of the Tunneling Channels of a Chemisorbed Molecule. *J. Phys. Chem. Lett.* **2010**, *1* (10), 1517–1523.
- (26) Grimme, S. Semiempirical GGA-Type Density Functional Constructed With a Long-Range Dispersion Correction. *J. Comput. Chem.* **2006**, *27* (15), 1787–1799.
- (27) Perdew, J. P.; Burke, K.; Ernzerhof, M. Generalized Gradient Approximation Made Simple. *Phys. Rev. Lett.* **1996**, *77* (18), 3865.
- (28) Eichkorn, K.; Weigend, F.; Treutler, O.; Ahlrichs, R. Auxiliary Basis Sets For Main Row Atoms and Transition Metals and Their Use to Approximate Coulomb Potentials. *Theor. Chem. Accounts: Theory, Comput., Model. (Theor. Chim. Acta)* **1997**, *97* (1), 119–124.
- (29) Eichkorn, K.; Treutler, O.; Öhm, H.; Häser, M.; Ahlrichs, R. Auxiliary Basis Sets to Approximate Coulomb Potentials (Chem. Phys. Letters 240 (1995) 283). *Chem. Phys. Lett.* **1995**, *242* (6), 652–660.
- (30) Ahlrichs, R.; Bar, M.; Häser, M.; Horn, H.; Kolmel, C. Electronic-Structure Calculations on Workstation Computers - The Program System Turbomole. *Chem. Phys. Lett.* **1989**, *162* (3), 165–169.
- (31) Andrae, D.; Haussermann, U.; Dolg, M.; Stoll, H.; Preuss, H. Energy-Adjusted Abinitio Pseudopotentials for the 2nd and 3rd Row Transition-Elements. *Theor. Chim. Acta* **1990**, *77* (2), 123–141.
- (32) Leung, K.; Rempe, S. B.; Schultz, P. A.; Sproviero, E. M.; Batista, V. S.; Chandross, M. E.; Medforth, C. J. Density Functional Theory and DFT+U Study of Transition Metal Porphyrins Adsorbed on Au(111) Surfaces and Effects of Applied Electric Fields. *J. Am. Chem. Soc.* **2006**, *128* (11), 3659–3668.
- (33) Hu, Z. P.; Li, B.; Zhao, A. D.; Yang, J. L.; Hou, J. G. Electronic and Magnetic Properties of Metal Phthalocyanines on Au(111) Surface: A First-Principles Study. *J. Phys. Chem. C* **2008**, *112* (35), 13650–13655.
- (34) da Silva, L.; Tiago, M. L.; Ulloa, S. E.; Reboredo, F. A.; Dagotto, E. Many-Body Electronic Structure and Kondo Properties of Cobalt-Porphyrin Molecules. *Phys. Rev. B* **2009**, *80* (15), 155443.
- (35) Zhang, Y. Y.; Du, S. X.; Gao, H. J. Binding Configuration, Electronic Structure, and Magnetic Properties of Metal Phthalocyanines on a Au(111) Surface Studied With Ab Initio Calculations. *Phys. Rev. B* **2011**, *84* (12), 125446.
- (36) Marom, N.; Kronik, L. Density Functional Theory of Transition Metal Phthalocyanines, I: Electronic Structure of NiPc and CoPc-Self-Interaction Effects. *Appl. Phys. A: Mater. Sci. Process.* **2009**, *95* (1), 159–163.
- (37) Cramer, C. J.; Truhlar, D. G. Density Functional Theory for Transition Metals and Transition Metal Chemistry. *Phys. Chem. Chem. Phys.* **2009**, *11* (46), 10757–10816.
- (38) Gargiani, P.; Calabrese, A.; Mariani, C.; Betti, M. G. Control of Electron Injection Barrier by Electron Doping of Metal Phthalocyanines. *J. Phys. Chem. C* **2010**, *114* (28), 12258–12264.
- (39) Perdew, J. P.; Ernzerhof, M.; Burke, K. Rationale for Mixing Exact Exchange with Density Functional Approximations. *J. Chem. Phys.* **1996**, *105* (22), 9982–9985.
- (40) VASP details: In the calculations of DOS of Ag(111) we perform VASP calculations within PAW methodology. The calculated lattice constant of bulk Ag is 4.109 and 4.110 Å for PBE and PBE0, respectively. For calculations of bulk (8,8,8), k-point sampling is used. For modeling Ag(111) surface 1 × 1, surface representation is used, and the periodically repeated slabs in normal direction to the surface are separated by 10 Å. The geometry optimization and DOS analysis of the Ag(111) surface is performed with (8,8,1) k-point mesh. The VASP plan-wave energy cutoff was 250 eV.
- (41) Kresse, G.; Hafner, J. Ab Initio Molecular Dynamics For Liquid Metals. *Phys. Rev. B* **1993**, *47* (1), 558–561.
- (42) Kresse, G.; Hafner, J. Ab Initio Molecular-Dynamics Simulation of the Liquid-Metal, Amorphous-Semiconductor Transition in Germanium. *Phys. Rev. B* **1994**, *49* (20), 14251–14269.

- (43) Kresse, G.; Furthmüller, J. Efficient Iterative Schemes for Ab Initio Total-Energy Calculations Using a Plane-Wave Basis Set. *Phys. Rev. B* **1996**, *54* (16), 11169–11186.
- (44) Kresse, G.; Furthmüller, J. Efficiency of Ab-Initio Total Energy Calculations for Metals and Semiconductors Using a Plane-Wave Basis Set. *Comput. Mater. Sci.* **1996**, *6* (1), 15–50.
- (45) Paier, J.; Marsman, M.; Kresse, G. Why Does the B3LYP Hybrid Functional Fail For Metals? *J. Chem. Phys.* **2007**, *127* (2), 024103–10.
- (46) Stroppa, A.; Kresse, G. The Shortcomings of Semi-Local and Hybrid Functionals: What We Can Learn From Surface Science Studies. *New J. Phys.* **2008**, *10* (6), 063020.
- (47) Baran, J. D.; Larsson, J. A.; Woolley, R. A. J.; Cong, Y.; Moriarty, P. J.; Cafolla, A. A.; Schulte, K.; Dhanak, V. R. Theoretical and Experimental Comparison of SnPc, PbPc, and CoPc Adsorption on Ag(111). *Phys. Rev. B* **2010**, *81* (7), 075413.
- (48) Skriver, H. L.; Rosengård, N. M. Surface Energy and Work Function of Elemental Metals. *Phys. Rev. B* **1992**, *46* (11), 7157–7168.
- (49) Salomon, E.; Amsalem, P.; Marom, N.; Vondracek, M.; Kronik, L.; Koch, N.; Angot, T. Electronic Structure of CoPc Adsorbed on Ag(100): Evidence for Molecule-Substrate Interaction Mediated by Co 3d Orbitals. *Phys. Rev. B* **2013**, *87* (7), 075407.
- (50) Gargiani, P.; Angelucci, M.; Mariani, C.; Betti, M. G. Metal-Phthalocyanine Chains On the Au(110) Surface: Interaction States Versus d-Metal States Occupancy. *Phys. Rev. B* **2010**, *81* (8), 085412.
- (51) Liao, M.-S.; Scheiner, S. Comparative Study of Metal-Porphyrins, -Porphyrazines, and -Phthalocyanines. *J. Comput. Chem.* **2002**, *23* (15), 1391–1403.
- (52) Mugarza, A.; Robles, R.; Krull, C.; Korytar, R.; Lorente, N.; Gambardella, P. Electronic and Magnetic Properties of Molecule-Metal Interfaces: Transition-Metal Phthalocyanines Adsorbed on Ag(100). *Phys. Rev. B* **2012**, *85* (15), 155437.
- (53) Schmid, M.; Kaftan, A.; Steinruck, H.-P.; Gottfried, J. M. The Electronic Structure of Cobalt(II) Phthalocyanine Adsorbed on Ag(111). *Surf. Sci.* **2012**, *606*, 945–949.
- (54) Lukaszczuk, T.; Flechtner, K.; Merte, L. R.; Jux, N.; Maier, F.; Gottfried, J. M.; Steinruck, H.-P. Interaction of Cobalt(II) Tetraarylporphyrins with a Ag(111) Surface Studied with Photoelectron Spectroscopy. *J. Phys. Chem. C* **2007**, *111* (7), 3090–3098.
- (55) Buchner, F.; Warnick, K. G.; Wölfe, T.; Gorling, A.; Steinruck, H. P.; Hieringer, W.; Marbach, H. Chemical Fingerprints of Large Organic Molecules in Scanning Tunneling Microscopy: Imaging Adsorbate-Substrate Coupling of Metalloporphyrins. *J. Phys. Chem. C* **2009**, *113* (37), 16450–16457.
- (56) Baran, J. D.; Larsson, J. A. Structure and Energetics of Shuttlecock-Shaped Tin-Phthalocyanine on Ag(111): A Density Functional Study Employing Dispersion Correction. *J. Phys. Chem. C* **2012**, *116* (17), 9487–9497.
- (57) Cuadrado, R.; Cerda, J. I.; Wang, Y. F.; Xin, G.; Berndt, R.; Tang, H. CoPc Adsorption on Cu(111): Origin of The C4 to C2 Symmetry Reduction. *J. Chem. Phys.* **2010**, *133* (15), 154701.
- (58) Bai, Y.; Buchner, F.; Kellner, I.; Schmid, M.; Vollnhals, F.; Steinruck, H. P.; Marbach, H.; Gottfried, J. M. Adsorption of Cobalt (II) Octaethylporphyrin and 2H-Octaethylporphyrin on Ag(111): New Insight Into the Surface Coordinative Bond. *New J. Phys.* **2009**, *11*, 125004.
- (59) Tosatti, E.; Fabrizio, M.; Tobik, J.; Santoro, G. E. Strong Correlations in Electron Doped Phthalocyanine Conductors Near Half Filling. *Phys. Rev. Lett.* **2004**, *93* (11), 117002.
- (60) Eremtchenko, M.; Schaefer, J. A.; Tautz, F. S. Understanding and Tuning the Epitaxy of Large Aromatic Adsorbates by Molecular Design. *Nature* **2003**, *425* (6958), 602–605.
- (61) Mercurio, G.; McNellis, E. R.; Martin, I.; Hagen, S.; Leyssner, F.; Soubatch, S.; Meyer, J.; Wolf, M.; Tegeder, P.; Tautz, F. S.; Reuter, K. Structure and Energetics of Azobenzene on Ag(111): Benchmarking Semiempirical Dispersion Correction Approaches. *Phys. Rev. Lett.* **2010**, *104* (3), 036102.
- (62) Marom, N.; Tkatchenko, A.; Rossi, M.; Gobre, V. V.; Hod, O.; Scheffler, M.; Kronik, L. Dispersion Interactions with Density-Functional Theory: Benchmarking Semiempirical and Interatomic Pairwise Corrected Density Functionals. *J. Chem. Theor. Comput.* **2011**, *7* (12), 3944–3951.